On the polarization of the green emission of polyfluorenes

X. H. Yang, D. Neher, C. Spitz, E. Zojer, J. L. Brédas et al.

Citation: J. Chem. Phys. **119**, 6832 (2003); doi: 10.1063/1.1605374
View online: http://dx.doi.org/10.1063/1.1605374
View Table of Contents: http://jcp.aip.org/resource/1/JCPSA6/v119/i13
Published by the American Institute of Physics.

On the polarization of the green emission of polyfluorenes

X. H. Yang, D. Neher,[a] and C. Spitz
University of Potsdam, Institute of Physics, Am Neuen Palais 10, 14469 Potsdam, Germany

E. Zojer[b]
Department of Chemistry, The University of Arizona, Tucson, AZ 85721-0041, and Institut für Festkörperphysik, Technische Universität Graz, A-8010 Graz, Austria

J. L. Brédas[b]
Department of Chemistry, The University of Arizona, Tucson, AZ 85721-0041

R. Güntner and U. Scherf
Bergische Universität Wuppertal, Fachbereich Chemie, Makromolekulare Chemie, Gauß-Str. 20, D-42097 Wuppertal, Germany

(Received 6 January 2003; accepted 10 July 2003)

An experimental and theoretical study of the anisotropic optical properties of polyfluorenes (PFs) bearing ketonic defects is presented. Polarized emission experiments performed on photooxidized aligned PF layers indicate that the transition dipole of the ''green'' CT π-π^* transition of the keto-defect is oriented parallel to the chain direction. It is further observed that the polarization ratio of the green emission is slightly smaller than that of the blue emission component originating from undisturbed chains. Quantum mechanical calculations have been performed to support these observations. It is shown that the transition dipole moment of the CT π-π^* transition of the defect is slightly misaligned with respect to the π-π^* transition of the undisturbed PF chain, and that the angle between both depends on the chain conformation. For the most probably 5/2 helical conformation, this angle is, however, smaller than 5°. Further, polarized PL spectroscopy with polarized excitation has been performed to determine the extent of energy migration prior to emission from the keto-defect. For excitation at 380 nm, the polarization ratio of the green emission is essentially independent of the excitation polarization, indicating almost complete depolarization of the excitation before it is captured at a defect site. In contrast to this, energy migration after direct excitation of the keto-defect is inefficient or even absent.
[DOI: 10.1063/1.1605374]

I. INTRODUCTION

Poly(alkylfluorene)s (PF) are a promising class of materials for optoelectronic and electronic applications.[1,2] PF has been extensively studied as the emissive material in blue light emitting diodes (LEDs)[3–6] or as host material for fluorescent and phosphorescent dyes.[7–9] Further, PF homo- and copolymers can be well aligned in the thermotropic liquid-crystalline state[10,11] and several applications have recently been demonstrated which exploit the anisotropy of the optoelectronic characteristics of the PF main chain. These include highly polarized light-emitting diodes,[6,12,13] field-effect transistors,[14] or polarization-sensitive photoconductors.[15,16] Therefore, the thermal and photochemical stability of polyfluorenes is a crucial issue concerning application of this interesting class of polymers.

Already the first paper on blue electroluminescence from PF reported an unwanted greenish emission in the electroluminescence spectra.[3] Several reports have later verified the existence of a broad green emission centered at ca. 530 nm in the photoluminescence and electroluminescence of polyfluorene homopolymer layers.[17–20] The relative intensity of this feature grows when the layer is either heated, irradiated with UV light or stressed by a large current in a LED device. Several approaches have been successfully applied to suppress the green emission such as narrowing the molecular weight dispersion,[20] adding hole-trapping molecules,[21] end-capping,[6,22] or dendronization.[23] In the past, mainly two models have been discussed to explain the origin of this emission: While earlier reports attributed the emission to the formation of excimers or aggregates,[19,24–26] recent papers presented convincing evidence that the introduction of fluorenone units (keto-defects) into the PF backbone either during polymerization or later by thermally or photoinduced reactions is the primary (and maybe exclusive) source of the green emission.[27–31]

However, none of the experimental and theoretical studies on the emission properties of the PF keto-defect have addressed the polarized optical properties. On the other hand, studies on macroscopically aligned polyfluorene layers[12] as well as microscopic fluorescence measurements utilizing scanning near-field optical microscopy (SNOM)[32] showed that the low energy emission is polarized along the same axis as the high energy blue emission from the radiative π-π^*

[a]Author to whom correspondence should be addressed. Electronic mail neher@rz.uni-potsdam.de
[b]Current address: School of Chemistry and Biochemistry, Georgia Institute of Technology, Atlanta, GA 30332-400.

transition of the polyfluorene backbone. It remains to be answered whether these observations are in accordance to the interpretation that the emission originates from keto-defects. In this article we investigate the polarized emission characteristics of keto-defects by studying the polarized photoluminescence of aligned polyfluorene samples after photooxidation in air. We observe that the low energy emission is only slightly less polarized than the blue band, and that the transition dipole moment of the green emission band lies basically parallel to the chain direction. Further, the extend of energy migration during photooxidation as well as in the course of excitation of the defect is investigated utilizing polarized excitation and emission spectroscopy on photooxidized aligned PF layers.

II. EXPERIMENTAL AND THEORETICAL METHODOLOGY

For our studies, an ethyl-hexyl substituted PF derivative (PF2/6bp7) endcapped with biphenyl at a molar ratio of 7% has been used (Scheme 1).[2]

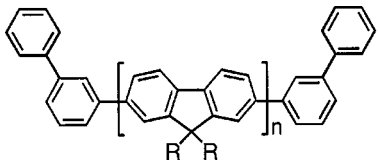

PF2/6bp7
(R: -2-ethylhexyl)

This derivative has a molecular weight $M_w = 38\,700$ g/mol, which allows for the alignment at moderate temperatures. Mondomain alignment of PF2/6bp7 was achieved on a 5–10 nm thick photoaligned layer of a photoaddressable polymer (PAP). Details on the preparation and photoalignment of the PAP layer can be found in our previous publications.[16,33,34] In brief, the PAP layer was spincoated from a 0.2 wt % solution of the polymer in THF at a spinning speed of 4500 rpm. After drying, this layer was illuminated with polarized light of an Ar^+ laser (intensity 150 mW/cm^2, wavelength 514 nm, illumination time 180 s), resulting in the alignment of the azobenzene side chains perpendicular to the polarization of the laser beam. Thereafter, a ca. 70 nm thick layer of PF2/6bp7 was spin-coated from toluene solution (concentration 1.2 wt %, spinning speed 1200 rpm) on top of the photoaligned PAP layer. Finally, the PF layer was aligned by annealing the sample at 125 °C for 3 min on a heat-plate in inert atmosphere.

Photooxidation was performed by irradiating the aligned sample in air with the unfocussed light of a 400 W xenon lamp. The intensity at the sample position was ca. 540 mW/cm^2.

Fluorescence excitation spectra were recorded with nonpolarized light using a Spex spectrometer equipped with a double-monochromator configuration for excitation and detection.

Polarized photoluminescence (PL) spectra were measured with a Perkin-Elmer luminescence spectrometer LS-50, equipped with a polarizer and an analyzer. PL spectra were recorded in a typical 90° reflection geometry with light incident to the layer at an incident angle of 60° with respect to the surface normal. Different combinations of the polarizer axis, the direction of the preferential chain alignment and the analyzer axis were used, namely HHH, HHV, VHH, VHV, VVV, VVH, HVV, HVH. Here, the first letter denotes the polarization of the excitation light (H: horizontal, V: vertical), the second the sample orientation, and the third the direction of the analyzer. All spectra were corrected for the wavelength and polarization sensitivity of the detection system and the intensity of the polarized excitation light.

For the quantum-mechanical simulations, the aliphatic side-chains attached to the carbon atoms in the bridge have been replaced by hydrogen as they do not directly affect the electronic structure of the π-conjugated backbone. The geometries of the molecules in their ground state are optimized with the semiempirical Hartree-Fock Austin Model 1 (AM1) method.[35] To account for the lattice relaxation in the excited state the AM1 Hamiltonian has been coupled to a multielectron configuration interaction (MECI) technique. A detailed discussion of the chosen CI space is given in Ref. 30. As aligned poly(fluorene)s with ethyl-hexyl side chains have been shown to crystallize in a 5/2 helix,[36] we have chosen a helical conformation here in which the bridges on neighboring fluorene units point in opposite directions. In the optimized conformation this yields a dihedral angle of 139° between two fluorene segments (as well as between fluorene segments and the fluorenone unit) in excellent agreement with the 144° that are to be expected for a perfect 5/2 helix. To study the effects of disorder also alternative geometries are considered. As model cases for deviations from a 5/2 helix, we have studied an alternating conformation and a chiral chain in which the bridges on adjacent fluorenes point in similar directions (i.e., close to a 5/1 helix). Transition energies and oscillator strengths are calculated on the basis of the semiempirical Hartree-Fock Intermediate Neglect of Differential Overlap (INDO) method[37,38] coupled to a single configuration interaction description including excitations from the sixty highest occupied to the sixty lowest unoccupied molecular orbitals.

III. RESULTS AND DISCUSSIONS

A. Polarized emission from the keto-defect

Figure 1(a) shows polarized PL spectra of an aligned PF sample before and after photooxidation for different periods of time. These spectra were recorded with nonpolarized excitation. The emission of the as-prepared sample shows a well-resolved structure with peaks at 424.5, 449, and 481 nm, assigned to the 0–0, 0–1, and 0–2 intra chain singlet transition, with the 0–0 transition being the most intense. The aligned layer exhibits a pronounced optical anisotropy as expressed by a large polarization ratio (defined as the ratio of intensity polarized parallel and perpendicular to the alignment direction) of 12–14 at 425 nm. The effect of illumination with Xe light in air is twofold: the intensity of the blue PF emission decreases drastically (not shown here) and a clearly resolved green emission band with a maximum at 530 nm emerges. Most important, the low energy emission is polarized parallel to the main alignment direction, as is confirmed by the wavelength dependence of the polarization ratio after different times of photooxidation displayed in Fig.

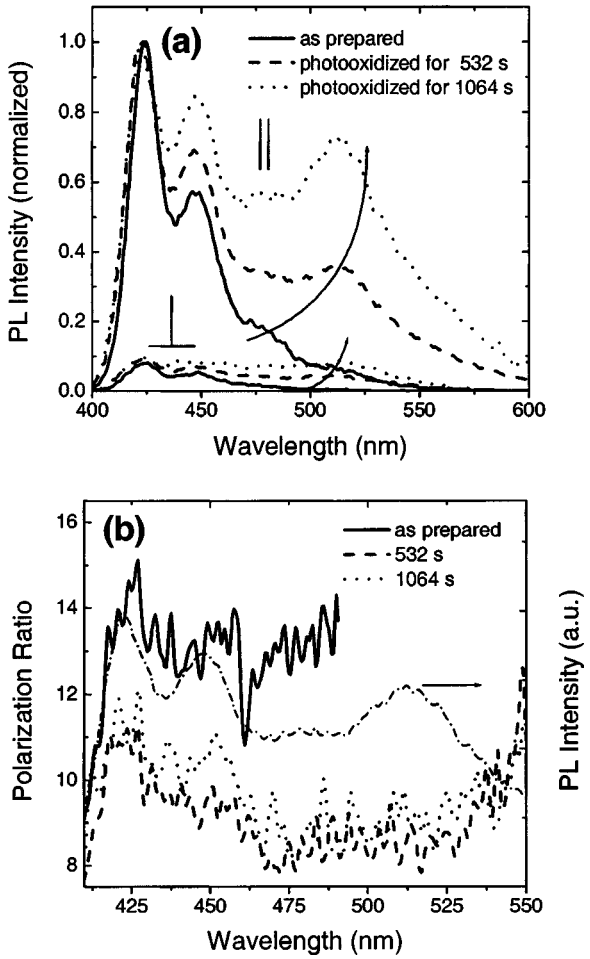

FIG. 1. Polarized photoluminescence spectra of an aligned polyfluorene sample before and after photooxidation. (a) shows data with the emission polarized parallel and perpendicular to the preferential chain alignment. Spectra have been corrected for the polarization sensitivity of the detection and normalized to the same intensity of the high energy emission peak in the parallel polarized spectra. The measurements were performed with nonpolarized excitation at 380 nm. The arrows indicate increasing illumination times. (b) shows the corresponding wavelength-dependent polarization ratios. The emission spectra of a layer photooxidized for 1064 s is shown for comparison.

1(b). This proves that the transitional dipole of the keto-defect is basically parallel to the chain direction. Therefore, the low energy emission contribution in the EL spectra of polarized light-emitting diodes and in the SNOM studies mentioned above can be fully explained by the polarized emission from keto-defects.

B. Evidence for energy migration during photooxidation

According to the data shown in Fig. 1(b), the polarization ratio of the polyfluorene emission of the photooxidized samples is slightly smaller than that of the pristine layers. This effect is well-reproducible, even for a photooxidation time of only 5 min (not shown here). Polarized and site-selective spectroscopy on aligned polyfluorene layers have shown that energy transfer primarily occupies chains which are oriented parallel to the alignment direction.[39] This has been explained by the angular dependence of energy transfer between two chains. One might, therefore, presume that well-aligned chains are the first to be photooxidized. However note, that we could not resolve any further decrease of the PF polarization ratio and of the anisotropy of the keto-emission for photoxidation times between 5 min and $\frac{1}{2}$ h within the experimental errors. We, therefore, conclude that energy transfer to highly aligned PF chains plays a role during photooxidation, but that the concentration of these chains in the sample is quite small.

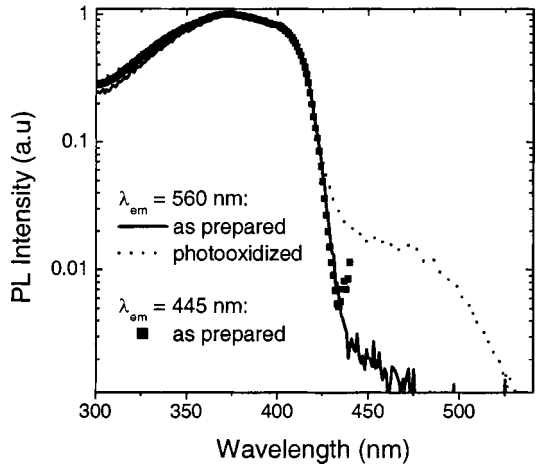

FIG. 2. Excitation spectra of an as-prepared sample and after photooxidation for 1–2 h. Spectra were recorded with an emission wavelength of 445 nm (squares) or 560 nm (lines).

C. Polarized emission spectroscopy

In order to probe the extent of depolarization and energy migration after excitation of a photooxidized sample, polarized emission spectra were recorded with polarized excitation either at the maximum of the polyfluorene π-π^* band (380 nm) or via direct excitation of the keto-defect (450 nm). As shown in Fig. 2, the excitation spectrum of a photooxidized sample measured with an emission wavelength of 560 nm exhibits a broad shoulder below the onset of the PF absorption, which is absent in the excitation spectrum of a nonphotooxidized layer. Based on experiments on poly(fluorene-co-fluorenone)[28] and theoretical studies,[30] this spectral feature can be assigned to the weak absorption of the CT π-π^* transition of the keto-defect. Apparently the keto-defect can be excited either directly or via the excitation of a singlet exciton on a nondisturbed PF chain followed by (inter- or intra-molecular) energy transfer. Nevertheless, the exciton on the keto-defect is more efficiently populated via the PF absorption, which is mainly due to the rather low oscillator strength of the CT π-π^* transition of the keto-defect. In fact, the emission intensity upon direct excitation of the keto-defect was very low (particularly for excitation polarized perpendicular to the chain alignment), and reliable data could be only obtained on samples, which had been photooxidized for at least 2 h.

Figure 3 shows the PL spectra of such a photooxidized sample measured with different combinations of the polarization of excitation, sample alignment and direction of the analyzer. We observe large differences between the absolute

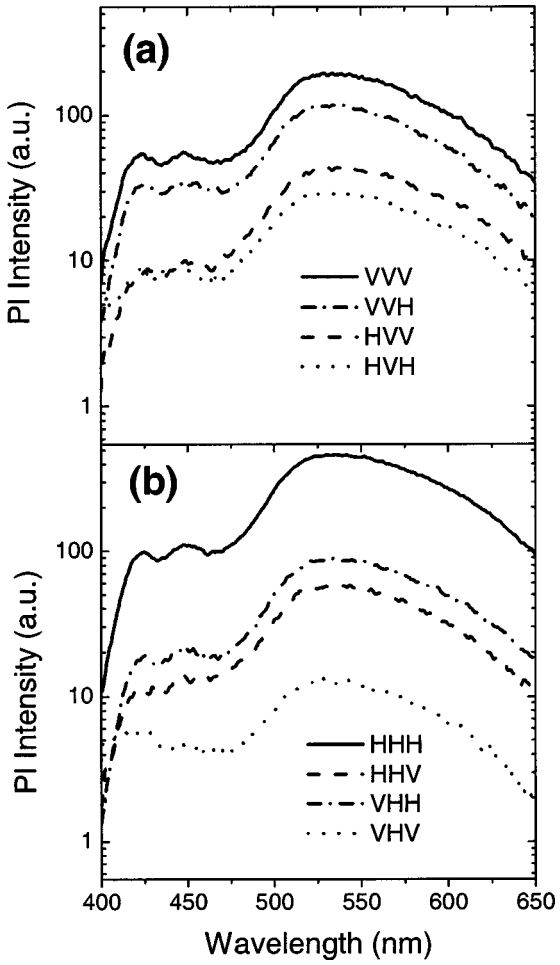

FIG. 3. Polarized photoluminescence spectra of a photooxidized aligned PF layer recorded with different combinations of the polarizer and the analyzer. The excitation wavelength was 380 nm. "V" and "H" denote a vertical and horizontal direction, respectively, of the polarizer, sample and analyzer. Spectra have been measured under otherwise identical conditions and corrected for the wavelength and polarization sensitivity of the detection.

emission intensities and polarization ratios for the two different sample orientations. This indicates that in addition to the intrinsic anisotropic optical properties of the PF layer, several additional factors affect the intensity of the detected polarized fluorescence light such as the transmission of the incident and emitted light through the air/polymer interface, interference effects or waveguiding within the PF layer. All of these contributions are expected to depend on the anisotropic refractive index of the aligned polymer layer and thus on the polarizations of the incident and emitted light with respect to the chain direction.

In a first approach we have corrected the spectra for the transmission T of $s(V)$- and $p(H)$-polarized light through the air/polymer interface according to Eqs. (1) and (2):

$$T_p = \left(\frac{n_t \cos\theta_t}{n_i \cos\theta_i}\right) t_p^2, \tag{1a}$$

$$T_s = \left(\frac{n_t \cos\theta_t}{n_i \cos\theta_i}\right) t_s^2, \tag{1b}$$

$$t_p = \frac{2 \sin\theta_t \sin\theta_i}{\sin(\theta_i + \theta_t)\cos(\theta_t - \theta_i)}, \tag{2a}$$

$$t_s = \frac{2 \sin\theta_t \cos\theta_i}{\sin(\theta_i + \theta_t)}. \tag{2b}$$

Here θ_i is the angle of incidence, θ_t is the angle of refraction, and n_i and n_t are the indices of refraction of the incident and transmitting medium, respectively. In the calculation of the transmission factors for the excitation light we assumed uniaxial birefringence. The refractive index dispersion for light polarized parallel ($n_\parallel$) and perpendicular ($n_\perp$) to the chain alignment was determined from a Kramers-Kronig analysis[40] of the polarized absorption spectra of an aligned PF2/6bp7 layer measured under normal incidence.

Since the excitation light is incident at a rather large angle of 60°, the refractive index for p-polarized light will be in-between the values of $n_\parallel$ and $n_\perp$. Therefore, in the calculation of the transmission coefficient for p-polarized incident light and horizontal sample orientation (HHH and HHV), we have determined the angle of refraction in the polymer layer and the corresponding refractive index by numerically solving Eq. (3):

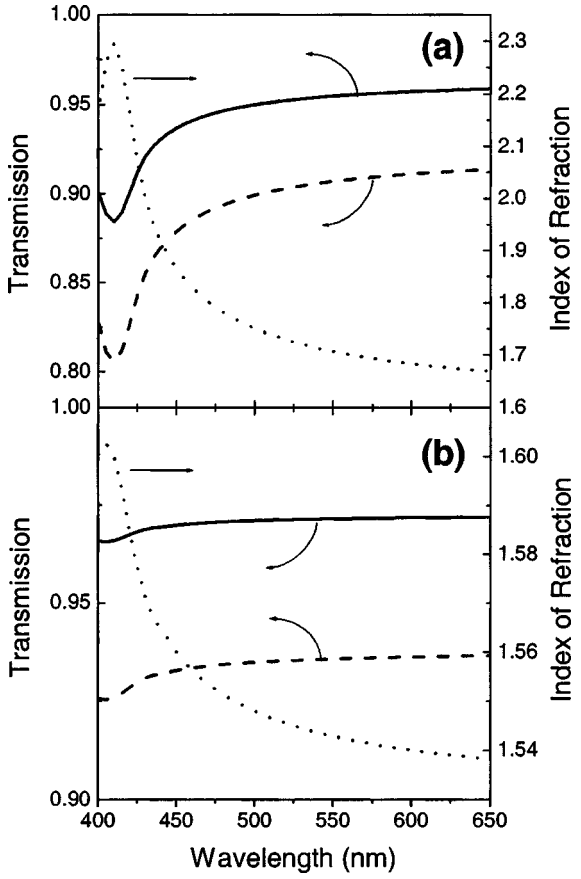

FIG. 4. Transmission coefficient as a function of wavelength used for the correction of the emission spectra, according to Eqs. (1)–(3). Transmission coefficients were calculated for p-polarized (solid line) and s-polarized (dashed line) emission, either polarized parallel (a) or perpendicular (b) to the chain alignment direction. The correction was based on the refractive index dispersions as shown with dotted lines, which were obtained from a Kramers-Kronig analysis of the polarized absorption spectra measured under normal incidence.

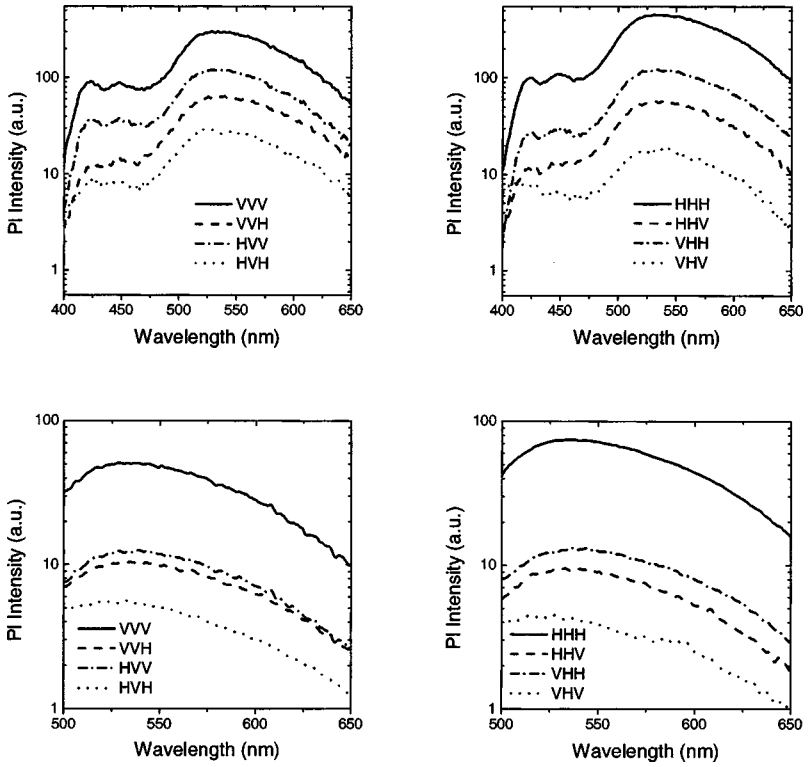

FIG. 5. Polarized emission spectra corrected for the transmission of the incident excitation light and the emitted light according to Eqs. (1)–(3) and Fig. 4. The upper graphs are for excitation at 380 nm, the lower for an excitation wavelength of 450 nm.

$$n_t = \frac{1}{\sqrt{\frac{\cos^2\theta_t}{n_\parallel} + \frac{\sin^2\theta_t}{n_\perp}}} = \frac{\sin\theta_i}{\sin\theta_t}. \tag{3}$$

Further, n_t was set equal to $n_\parallel$ for *s*-polarized excitation and vertical sample alignment (VVV,VVH), while $n_\perp$ was used if the incident light was polarized perpendicular to the chain alignment (HVH,HVV,VHH,VHV). Because the internal angle of the emitted light in the polymer layer is quite small (light was detected under an angle of 30° with respect to the surface normal), the transmission factors for emission were calculated using the corresponding in-plane values $n_\parallel$ and $n_\perp$.

The refractive index dispersions for light polarized parallel and perpendicular to the alignment direction as well as the wavelength dependent transmission coefficients for emission are shown in Fig. 4. The shapes of the dispersion curves and the absolute values of the refractive indices compare quite well to those recently measured on a layer with preferential in-plane orientation of PF chains, utilizing spectral ellipsometry.[41] Apparently there is a significant difference in the transmission coefficients for light polarized in the H and V direction. Throughout the entire wavelength range, the transmission for H-polarized excitation and emission is close to one, which is due to the fact that the incident angles are close to the Brewster angle.

Figure 5 shows the corrected emission spectra. For both excitation wavelengths, the spectra measured with vertical and horizontal sample orientation compare quite well. The rather good agreement between the spectra measured with different sample orientation is quite surprising, since several simplifications have been made in the correction and any thin-film effects have been neglected. Nevertheless, data recorded with vertical sample orientation and particularly those measured with *s*-polarized emitted light consistently yield slightly lower intensities. While part of this difference might be due to the fact that the sample had to be removed and re-inserted into the sample holder in order to change its orientation, we presume that multiple reflection in the polymer layer (which is expected to be more prominent for *s*-polarized light) does further affect the emitted signal intensity.

The polarization ratios (averages of the ratios measured with horizontal and vertical sample orientation) at 425, 450,

TABLE I. Polarization ratio of photoluminescence measured on an aligned photooxidized PF-sample at different emission wavelengths. The excitation wavelength was 380 nm or 450 nm and the polarization of the excitation light was either parallel or perpendicular to the direction of preferential chain alignment. The listed values are averages of the ratios measured for vertical and horizontal sample alignment.

Excitation	$\lambda_{em}=422$ nm	$\lambda_{em}=450$ nm	$\lambda_{em}=550$ nm
		$\lambda_{ex}=380$ nm	
∥-chains	8.1±0.6	7.4±0.7	6.4±1.7
⊥-chains	⋯	5.3±0.6	5.3±1.1
		$\lambda_{ex}=450$ nm	
∥-chains			6.4±1.6
⊥-chains			2.9±0.4

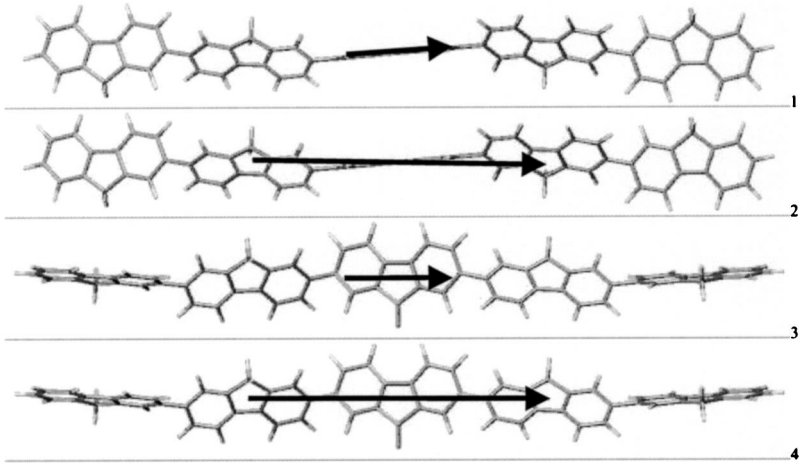

FIG. 6. INDO/SCI calculated transition dipoles for the ground to CT π-π^* (1,3) and ground to π-π^* excitations (2,4) in the 5/2 helical conformation. In 3 and 4 the molecule has been rotated by 90°.

and 540 nm are listed in Table I. Note that the intensity of the polarized emission for perpendicular excitation and emission was very low for both sample orientations and there is a significant background in the high-energy part of the spectra caused by stray light from the single-monochromator excitation unit. Therefore, values of the polarization ratio for perpendicular excitation are only given for wavelengths well below the excitation wavelength.

D. Depolarization after excitation

There is a remarkably small dependence of the polarization ratio of the keto-emission on the polarization of the excitation light if the sample is excited at 380 nm. Obviously, the excitation depolarizes almost completely before being captured at a keto-defect. In contrast to that, the polarization ratio depends significantly on the polarization of the excitation light if the layer is excited at 450 nm (see Table I) The polarization ratio drops by a factor of more than 2 when the excitation is switched from parallel to perpendicular excitation. Obviously, depolarization is far less pronounced or even absent if the keto-defect is excited directly. This is mainly caused by the fact that excitation at 450 nm is ca. 0.2 eV below the delocalization threshold of polyfluorene at 2.97 eV (measured at 77 K)[39] and exciton migration thus requires thermal activation. Moreover, geometrical relaxation of the keto-defect in its excited state is expected to further lower the energy and trap the excitation at the defect.[30] Therefore, the excitation is expected to remain on the originally excited keto-site, provided that the concentration of keto-defects in the photooxidized samples is too low to facilitate direct exciton transfer between fluorenone groups. A quantitative analysis of the (possible) extend of energy transfer for excitation at 450 nm would, however, require the exact knowledge of the orientational distribution function which is not known to us for the present sample.

E. Quantum-mechanical calculations

In order to better understand the relative polarizations of the various excitations in poly(fluorene)s containing keto-defects, quantum-mechanical calculations have been performed on model systems containing four fluorene units and a fluorenone segment. The electronic structure of the helical conformation is equivalent to that of the alternating conformation discussed in detail in Ref. 30. We find three low-lying excited states, namely an optically forbidden n-π^* excited state, a weakly allowed charge-transfer (CT) π-π^* excited state (that is responsible for the green emission of the keto-defect) and a strongly allowed π-π^* excited state reminiscent of the lowest lying excited state in pristine poly(fluorene). In the ground state conformation (i.e., for absorption processes), the n-π^* state is lowest in energy. This changes in the relaxed excited state geometry (i.e., for the emission process), resulting in the greenish emission from the CT π-π^* state.[30] In this contribution we are mainly concerned with the polarization of the various optically allowed excited states. Therefore, the transition dipole moment vectors for the ground to CT π-π^* and ground to π-π^* excitations are shown in Fig. 6 for the 5/2 ground state conformation. They are virtually parallel (angle of 2.8° between the two vectors) and this hardly changes when moving the fluorenone unit from the center of the model molecule to its extremities (see Table II). The upper part of Fig. 6 indicates that the slight misalignment is caused by the ground to CT π-π^* transition dipole moment being parallel to the fluorenone unit, while the ground to π-π^* transition dipole is parallel to the ''rest'' of the molecule. A similar behavior is observed for the alter-

TABLE II. INDO/SCI calculated transition dipoles for the ground to CT π-π^* ($M_{\mathrm{CT}\pi\text{-}\pi^*}$) and ground to π-π^* ($M_{\pi\text{-}\pi^*}$) excitations for various conformations (a model system containing five fluorene and one fluorenone unit has been chosen). In parentheses the values for relaxed excited state geometries are given for selected conformations.

Pos. of fluorenone unit	$M_{\mathrm{CT}\text{-}\pi\text{-}\pi^*}$ (debye)	$M_{\pi\text{-}\pi^*}$ (debye)	Angle between $M_{\mathrm{CT}\text{-}\pi\text{-}\pi^*}$ and $M_{\pi\text{-}\pi^*}$
''5/2 helix'':			
left	4.4	17.1	5.0°
2nd segment	5.5	16.2	1.5°
center	5.9 (7.0)	16.7 (15.4)	2.8°(1.7°)
''5/1 helix'':			
left	4.3 (4.7)	16.2 (16.0)	24.9°(21.0°)
center	5.7	15.6	6.5°
alternating:			
left	4.4 (5.1)	17.0 (16.1)	11.5°(7.5°)
center	5.9 (7.0)	16.6 (15.3)	0.0°(0.0°)

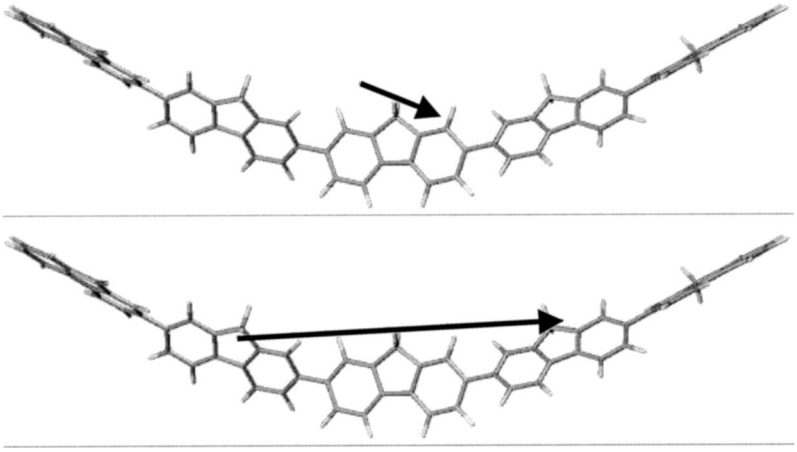

FIG. 7. INDO/SCI calculated transition dipoles for the ground to CT π-π^* (top) and ground to π-π^* excitations (bottom) in the 5/1 helical conformation with the fluorenone unit located at the left end of the molecule.

nating conformation (see Table II). As a more extreme type of distortion we have also considered a situation reminiscent of a 5/1 helical conformation. Here, the misalignment between the transition dipoles can become quite large, especially if the fluorenone unit is at the extremity of the molecule. The obtained orientation of the transition dipoles for a terminal fluorenone unit (shown in Fig. 7) confirms the assumption that the transition dipole to CT π-π^* is determined by the local orientation of the fluorenone unit, while the dipole coupling of the π-π^* excited state with the ground state follows the direction of the π-electron system in the nonsubstituted fluorene chain. As a result, variations of the local alignment of the fluorenone units can result in somewhat different angles between the transition dipoles obtained for various defect positions and chain conformations. Based on these results we conclude that the smaller polarization ratio of the keto-emission [compared to the emission form the undisturbed chains; see, e.g., Fig. 1(b)] is mainly caused by disorder effects rather than by the small misalignment of the CT π-π^* transition dipole of an ideal chain in the 5/2 conformation.

F. Alignment of the CT π^*-π dipole moment in the excited state configuration

Finally, we would like to comment on the misalignment of the CT π^*-π dipole moment in the relaxed excited state geometry, compared to that in the ground state configuration. Unfortunately, it was not possible to determine the dichroic ratio of the CT π-π^* transition in absorption (due to the very weak signal for the perpendicular absorption). But we like to point out that in case of direct excitation of the keto-defect at 450 nm, the emission intensity measured in the VVH geometry was almost the same as that measured for HVH (the intensities measured in the HHV and VHH geometry were also comparable). This provides experimental evidence that the misalignment of the transition dipole moment of the CT π^*-π transition in the ground state geometry and in the relaxed excited state configuration is basically identical.

This interpretation is supported by the results of quantum mechanical calculations. For the relaxed excited state geometries (values in parentheses in Table II), we observe a minor redistribution of oscillator strength to the CT π-π^* state and smaller angles between the transition dipoles. This is due to a reduction of the dihedral angles between the fluorenone units and the neighboring fluorene segments, which reduces the misalignment of the fluorenone relative to the rest of the polymer (torsions are reduced from 41° in the ground state conformation to values between 25° and 29° depending on the molecular conformation). We like to point out that one obtains virtually the same relative orientation of $M_{\mathrm{CT}\text{-}\pi\text{-}\pi^*}$ and $M_{\pi\text{-}\pi^*}$ in the excited and ground state conformations, if one set the torsion angles in the excited state back to the values for the ground state geometry. For the thin film samples investigated here, one might, in fact, expect an intermediate scenario, as the change of the torsion between fluorene and fluorenone segments should be strongly reduced as a consequence of intermolecular packing forces and the interaction between the side chains.

IV. CONCLUSION

Based on the results of our studies of the polarized emission properties of photooxidized aligned polyfluorene layers the following conclusions can be drawn: When the sample is excited 380 nm, at the maximum of the lowest lying π-π^* transition of the undisturbed PF chain, emission is observed from both the singlet exciton on the PF chain as well as from the CT-exciton on the keto-defect. The polarized emission exhibits a pronounced optical anisotropy throughout the whole spectrum, proving that the transition dipole of the CT π-π^* transition of the keto-defect is oriented largely parallel to the chain direction. However, the emission from the keto-defect exhibits a somewhat smaller polarization ratio than the blue emission from the defect-free chains. This can be understood in the light of the quantum-mechanical simulations, which show that the polarization of the fluorenone emission is influenced by local disorder. The polarization of the low-energy emission is almost not depending on the polarization of excitation if the sample is excited at 380 nm. This suggests an almost complete depolarization of excitation before it is captured by a keto-defect. In contrast to that, the polarization ratio of the green emission depends significantly on the polarization of the exciting light for an excitation wavelength of 450 nm, indicating that energy migration after direct excitation of the keto-defect is inefficient or even absent. This suggests that the energy of the excited state of

the keto-defect is below the delocalization threshold of polyfluorene. Finally, we note that earlier reports on the polarization of green emission in ordered or aligned PF layers are in accordance with the interpretation that this emission originates from the weakly allowed transition of PF chains carrying ketonic units.

ACKNOWLEDGMENTS

Financial support by the German Ministry of Science and Education, by the *Fond der Chemischen Industrie* and the *Spezialforschungsbereich Elektroaktive Stoffe* is acknowledged. The authors would like to thank J.-P. Calbert for providing the ZOA data analysis program. The work in Arizona has been partly supported by the National Science Foundation (CHE-0078819), the IBM Shared University Research program, and the College of Science of the University of Arizona.

[1] D. Neher, Macromol. Rapid Commun. **22**, 1366 (2001).
[2] U. Scherf and E. J. W. List, Adv. Mater. **14**, 477 (2002).
[3] Y. Ohmori, M. Uchida, K. Muro, and K. Yoshino, Jpn. J. Appl. Phys. **30**, 1941 (1991).
[4] A. W. Grice, D. D. C. Bradley, M. T. Bernius, M. Inbasekaran, W. W. Wu, and E. P. Woo, Appl. Phys. Lett. **73**, 629 (1998).
[5] M. Gross, D. C. Muller, H. G. Nothofer, U. Scherf, D. Neher, C. Brauchle, and K. Meerholz, Nature (London) **405**, 661 (2000).
[6] T. Miteva, A. Meisel, W. Knoll, H. G. Nothofer, U. Scherf, D. C. Müller, K. Meerholz, A. Yasuda, and D. Neher, Adv. Mater. **13**, 565 (2001).
[7] T. Virgili, D. G. Lidzey, and D. D. C. Bradley, Adv. Mater. **12**, 58 (2000).
[8] T.-F. Guo, S.-S. Chang, Y. Yang, R. C. Kwong, and M. E. Thompson, Org. Electronics **1**, 15 (2000).
[9] V. Cleave, G. Yahioglu, P. Le Barny, D. H. Hwang, A. B. Holmes, R. H. Friend, and N. Tessler, Adv. Mater. **13**, 44 (2001).
[10] M. Grell, D. D. C. Bradley, M. Inbasekaran, and E. P. Woo, Adv. Mater. **9**, 798 (1997).
[11] M. Grell, M. Redecker, K. S. Whitehead, D. D. C. Bradley, M. Inbasekaran, E. P. Woo, and W. Wu, Liq. Cryst. **26**, 1403 (1999).
[12] M. Grell, W. Knoll, D. Lupo, A. Meisel, T. Miteva, D. Neher, H. G. Nothofer, U. Scherf, and A. Yasuda, Adv. Mater. **11**, 671 (1999).
[13] K. S. Whitehead, M. Grell, D. D. C. Bradley, M. Jandke, and P. Strohriegl, Appl. Phys. Lett. **76**, 2946 (2000).
[14] H. Sirringhaus, R. J. Wilson, R. H. Friend, M. Inbasekaran, W. Wu, E. P. Woo, M. Grell, and D. D. C. Bradley, Appl. Phys. Lett. **77**, 406 (2000).
[15] F. C. Grozema, T. J. Savenije, M. J. W. Vermeulen, L. D. A. Siebbeles, J. M. Warman, A. Meisel, D. Neher, H. G. Nothofer, and U. Scherf, Adv. Mater. **13**, 1627 (2001).
[16] A. Zen, D. Neher, C. Bauer, U. Asawapirom, U. Scherf, R. Hagen, S. Kostromine, and R. F. Mahrt, Appl. Phys. Lett. **80**, 4699 (2002).
[17] Q. B. Pei and Y. Yang, J. Am. Chem. Soc. **118**, 7416 (1996).
[18] J. I. Lee, G. Klaerner, and R. D. Miller, Synth. Met. **101**, 126 (1999).
[19] V. N. Bliznyuk, S. A. Carter, J. C. Scott, G. Klärner, R. D. Miller, and D. C. Miller, Macromolecules **32**, 361 (1999).
[20] K. H. Weinfurtner, H. Fujikawa, S. Tokito, and Y. Taga, Appl. Phys. Lett. **76**, 2502 (2000).
[21] D. Sainova, T. Miteva, H. G. Nothofer, U. Scherf, I. Glowacki, J. Ulanski, H. Fujikawa, and D. Neher, Appl. Phys. Lett. **76**, 1810 (2000).
[22] J. I. Lee, D. H. Hwang, H. Park, L. M. Do, H. Y. Chu, T. Zyung, and R. D. Miller, Synth. Met. **111**, 195 (2000).
[23] S. Setayesh, A. C. Grimsdale, T. Weil, V. Enkelmann, K. Müllen, F. Meghdadi, E. J. W. List, and G. Leising, J. Am. Chem. Soc. **123**, 946 (2001).
[24] J. I. Lee, G. Klärner, and R. D. Miller, Chem. Mater. **11**, 1083 (1999).
[25] J. Teetsov and M. A. Fox, J. Mater. Chem. **9**, 2117 (1999).
[26] L. M. Herz and R. T. Phillips, Phys. Rev. B **61**, 13691 (2000).
[27] E. J. W. List, R. Güntner, P. S. de Freitas, and U. Scherf, Adv. Mater. **15**, 374 (2002).
[28] P. Scandiucci de Freitas, U. Scherf, M. Collon, and E. J. W. List, e-Polymers **9**, 1 (2002).
[29] J. M. Lupton, M. R. Craig, and E. W. Meijer, Appl. Phys. Lett. **80**, 4489 (2002).
[30] E. Zojer, A. Pogantsch, E. Hennebicq, D. Beljonne, J. L. Bredas, P. S. de Freitas, U. Scherf, and E. J. W. List, J. Chem. Phys. **117**, 6794 (2002).
[31] X. Gong, P. K. Iyer, D. Moses, G. C. Bazan, A. J. Heeger, and S. S. Xiao, Adv. Funct. Mater. **13**, 325 (2003).
[32] J. Teetsov and D. A. Vanden Bout, J. Phys. Chem. B **104**, 9378 (2000).
[33] D. Sainova, A. Zen, H.-G. Nothofer, U. Asawapirom, U. Scherf, R. Hagen, T. Bieringer, S. Kostromine, and D. Neher, Adv. Funct. Mater. **12**, 49 (2002).
[34] X. H. Yang, D. Neher, S. Lucht, H. Nothofer, R. Guntner, U. Scherf, R. Hagen, and S. Kostromine, Appl. Phys. Lett. **81**, 2319 (2002).
[35] M. J. S. Dewar, E. G. Zoebisch, E. F. Healy, and J. J. P. Stewart, J. Am. Chem. Soc. **107**, 3902 (1985).
[36] G. Lieser, M. Oda, T. Miteva, A. Meisel, H. G. Nothofer, U. Scherf, and D. Neher, Macromolecules **33**, 4490 (2000).
[37] J. E. Ridley and M. C. Zerner, Theor. Chim. Acta **42**, 223 (1976).
[38] M. C. Zerner, G. H. Loew, R. F. Kirchner, and U. T. Muellerwesterhoff, J. Am. Chem. Soc. **102**, 589 (1980).
[39] C. Bauer, G. Urbasch, H. Giessen, A. Meisel, H. G. Nothofer, D. Neher, U. Scherf, and R. F. Mahrt, ChemPhysChem **1**, 142 (2000).
[40] V. Cimrova, D. Neher, S. Kostromine, and T. Bieringer, Macromolecules **32**, 8496 (1999).
[41] M. Tammer, R. W. T. Higgins, and A. P. Monkman, J. Appl. Phys. **91**, 4010 (2002).